FACTA UNIVERSITATIS
Series: **Mechanical Engineering**
https://doi.org/10.22190/FUME260410011M

Original scientific paper

HAIL IMPACT RESISTANCE OF NEXT-GENERATION LIGHTWEIGHT PHOTOVOLTAIC MODULES REINFORCED WITH HONEYCOMB SANDWICH STRUCTURES

Vytautas Makarskas[1], Egidijus Dragašius[1], Jonas Matijošius[2], Kristina Kilikevičienė[2], Artūras Kilikevičius[2], Miloš Milovančević[2]

[1]Department of Production Engineering, Faculty of Mechanical Engineering and Design, Kaunas University of Technology, Lithuania
[2]Mechanical Science Institute, Vilnius Gediminas Technical University, Vilnius, Lithuania

Abstract. *The demand for lightweight photovoltaic (PV) modules is increasing due to the expansion of building-integrated and mobile PV applications, where conventional glass-based modules are limited by weight and rigidity. Honeycomb sandwich reinforcement offers high stiffness-to-weight ratio. However, its dynamic response under extreme impact loading remains insufficiently understood. This study outlines both experimental and numerical investigations of a flexible photovoltaic module enhanced by a honeycomb structure. An experimental modal analysis was conducted to determine natural frequencies and mode shapes, alongside the creation and validation of a finite element model, which showed eigenfrequency deviations below 10% for the first four modes, with most modes remaining below approximately 7%. The validated model was subsequently utilized to simulate the impacts of hail and evaluate the distribution of stress across the multilayer structure. The peak von Mises stresses were localized within the brittle silicon solar cell layer. In contrast to the non-reinforced configuration, the honeycomb-reinforced module demonstrated marginally elevated peak stresses, reaching approximately 149 MPa, which can be ascribed to enhanced structural stiffness and diminished global deformation. The suggested methodology offers a profound understanding of stress transfer mechanisms in lightweight photovoltaic modules and facilitates structural optimization aimed at enhancing hail resistance.*

Key words: *Lightweight photovoltaic modules, Honeycomb sandwich structures, Dynamic parameters, Hail impact*

Received: April 10, 2026 / Accepted July 3, 2026
Corresponding author: Jonas Matijošius
Mechanical Science Institute, Vilnius Gediminas Technical University, Plytinės Str. 25, LT-10105 Vilnius, Lithuania
E-mail: jonas.matijosius@vilniustech.lt

© 2026 by University of Niš, Serbia | Creative Commons License: CC BY-NC-ND

1. INTRODUCTION

In recent years, the deployment of photovoltaic (PV) modules has grown rapidly worldwide, but at the same time, the challenges related to their long-term reliability under extreme environmental conditions are increasing. Climatic differences determine both the degradation mechanisms and their rate, which is directly reflected in the changes in current (ISC), voltage (VOC), fill factor (FF) and power (P_{max}) [1]. Regions with increasing frequency of extreme hydroclimatic events, including hail, which is considered one of the most dangerous shock effects for PV systems, are becoming particularly relevant. Hail risk assessment has recently moved from simple geostatistical assessments to spatiotemporally detailed models that allow predicting the probability, size and frequency of hail in specific locations [2]. It has been found that in some regions, during a typical 25-year service life of a PV module [3], dozens of episodes may occur, when more than 11 hailstones with a diameter exceeding 50 mm reach an area of 1 m² per minute [4]. Such conditions significantly exceed the typical loads of laboratory tests defined in the IEC 61215 standard [5, 6].

Laboratory and field studies show that the outcome of a hail impact strongly depends on the thickness of the windshield, the speed and mass of the ice ball [7]. However, it is increasingly emphasized that not only the glass, but also other elements of the multilayer structure – encapsulation, back layer, cell arrangement – have a significant impact on the resistance [8]. This indicates that the impact mechanics must be assessed at the level of the entire laminated structure, and not only at the level of the surface glass.

The nature of dynamic loading is examined in detail in experimental studies of the mechanical properties of ice using the Split Hopkinson Pressure Bar method [9]. It has been found that the size, speed, temperature and impact angle of the ice ball directly affect the maximum peak load and pulse duration [10]. Lower ice temperature leads to higher impact force and shorter peak time, and changes in the angle modify the maximum load. This confirms that hail modeling must include dynamic, not just static analysis. High-speed video analysis allows for a more accurate assessment of the temporal structure of the impact process. Laboratory tests have shown that glass breakage occurs even when the stress concentration remains localized in the impact zone, and the stress levels exceed the limits of static fracture [11]. This confirms that glass breakage is a time- and velocity-dependent process, and therefore the application of structural strength criteria alone may not be sufficient [12].

In addition to glass damage, the formation of microcracks in solar cells is also of critical importance. Even in the absence of obvious glass breakage, electroluminescence (EL) and infrared (IR) studies reveal hidden defects that can eventually lead to local overheating and safety risks [13]. It has been found that even without glass breakage, defects can form in the cells that cannot be detected with the naked eye, but they manifest themselves as reduced EL intensity and increased thermal emission [14].

Different types of modules react differently to hail. Experimental studies show that monocrystalline modules have better resistance than polycrystalline ones, and the power loss after impact can reach 4.15% and 12.59%, respectively [15]. It has also been found that edge impacts cause damage at lower energy than central impacts, and glass/glass structures with thinner tempered glass may be less resistant than glass/backsheet solutions [16].

From a mechanical point of view, the role of the mounting configuration is also important. Numerical simulations show that an optimal horizontal support distance ratio (~0.21 module length) allows to reduce the principal stress values and crack propagation

[17]. Similarly, cyclic loading analysis reveals that crack growth accelerates at load amplitudes above 1500 Pa, and the way the modules are mounted determines the time of crack initiation and propagation [18].

In the context of lightweight and semi-flexible modules, it has been found that traditional laminated panel theory can significantly overestimate or underestimate stresses and strains compared to finite element modeling [19]. This shows that accurate dynamic analysis is necessary, especially for the next generation of lightweight structures [20], while isogeomtric FE approach is particularly promising for thin-walled structures [21].

In addition to mechanical aspects, environmental effects are also important. UV radiation is considered one of the main degradation initiation factors, causing yellowing, delamination and optical losses of the encapsulant [22]. The proposed degradation severity index (DSI) allows for the quantitative assessment of the importance of different defects by integrating degradation rate, impact weight, and material sensitivity.

Meanwhile, advanced encapsulation strategies, such as multifunctional layers based on natural shellac, allow achieving compliance with IEC 61215 requirements, including hail tests [23]. This shows that structural solutions can be an effective way to increase resistance [24].

Fault detection is becoming an integral part of reliability assessment. EL, IR and UV fluorescence methods allow for the detection of hidden defects even with minimal power loss [25]. At the same time, machine learning models are being developed to automate fault detection in large solar power plants [26].

From an economic point of view, the cost of replacing a module due to glass breakage and hail can reach 1–5% of the total system value, therefore, structural preventive measures (thicker glass, stronger frames) can be economically justified if their cost does not exceed these losses [27].

Summarizing the literature, it can be stated that the impact of hail on PV modules is a multifaceted phenomenon, including dynamic impact mechanics, stress redistribution of the multilayer structure, crack initiation of the brittle silicon cell and long-term degradation. Despite extensive research, there remains a gap between experimental tests and validated numerical models that could accurately reflect real loads and structural configurations. In particular, there is a lack of research combining dynamic modal characterization with hail impact modeling in lightweight, non-standard structures.

It is this gap that justifies the need to apply an experimental-numerical methodology that allows for the validation of the dynamic model before performing impact analysis, and forms the basis for further structural optimization to increase the resistance of lightweight PV modules to extreme climatic loads.

This study presents a unique approach by combining experimentally validated modal analysis with simulations of transient hail impacts on honeycomb-reinforced lightweight photovoltaic modules. This research diverges from traditional investigations that emphasize glass-based modules or solely numerical impact assessments, illustrating instead the significant role of dynamic stiffness characteristics in shaping stress transmission mechanisms within multilayer flexible photovoltaic structures. The findings elucidate a stress amplification phenomenon induced by stiffness within the brittle silicon layer, offering fresh perspectives on the mechanical design considerations inherent in sandwich-reinforced photovoltaic modules.

2. MATERIALS AND METHODS

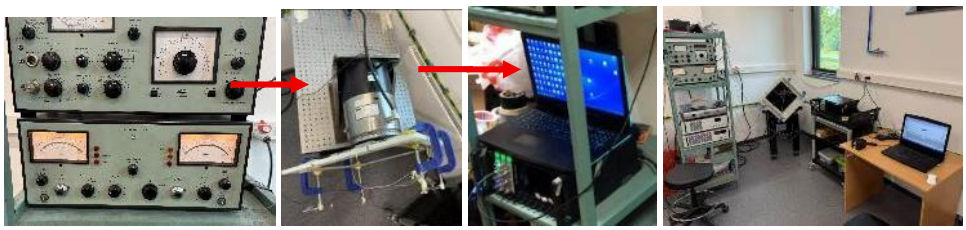
Modal analysis was performed to characterize the dynamic response of a lightweight flexible photovoltaic (PV) module reinforced with a honeycomb (HC) sandwich structure. The main goal of the study was to identify the key modal parameters: natural frequencies, mode shapes, and modal damping ratios, which are essential for accurate prediction of structural behavior under dynamic mechanical excitation and for subsequent impact simulations (hail loading). Modal parameters represent fundamental indicators of structural stiffness distribution, mass effects, and boundary condition sensitivity [28].

In the context of honeycomb-based PV modules, modal characterization is particularly important because sandwich structures typically exhibit strong orthotropic stiffness properties, complex local deformation patterns, and frequency-dependent energy dissipation mechanisms. Therefore, reliable identification of the dynamic properties is required to establish a validated mechanical model capable of predicting stress concentrations and potential failure zones under transient impact events.

To ensure the robustness of the obtained results, both experimental modal analysis and numerical (FE-based) modal analysis were conducted. Six PV module specimens with honeycomb reinforcement were tested experimentally, and their results were compared with the numerical predictions. The FE model was iteratively updated until sufficient correlation between experimental and numerical modal parameters was achieved.

The overall methodology applied in this research is summarized in Fig. 1 (conceptual workflow) and consists of four main stages:

1. Experimental modal testing (Fig. 1) of the PV module with honeycomb reinforcement to obtain response signals and determine modal parameters.
2. Numerical FE model development, including geometry definition, material property assignment, and boundary condition implementation.
3. Model validation and updating, where FE parameters were tuned until acceptable agreement was reached. The validated FE model was then adopted for subsequent impact simulations (hail loading scenarios).



a) b) c) d)

Fig. 1 Bench for determining the dynamic characteristics of a flexible PV module:
a) Generating an excitation signal, b) Measurement of the objects response,
c) Measurement data collection, d) The entire setup

This integrated approach ensures that the numerical model is not purely theoretical but reflects the real dynamic behavior of the tested PV module, making it suitable for further mechanical stress and damage analysis.

Table 1 summarizes the key material properties adopted in the 2D finite element model, including density, Young's modulus, and Poisson's ratio, which were required to represent

the mechanical response of the multilayer PV structure under hail impact loading. The numerical model incorporated the main functional layers of the lightweight PV module, namely the PET-based frontsheet, EVA encapsulation, monocrystalline silicon solar cell layer, and a polypropylene (PP) honeycomb core represented as an equivalent homogenized layer. In addition, the impacting hailstone was modeled as an ice sphere with material parameters consistent with commonly reported values in hail impact simulations. The thicknesses of the modeled PV layers were defined according to the module architecture: PET – 0.22 mm, EVA – 0.5 mm, solar cell – 0.17 mm, and honeycomb reinforcement – 12 mm, while the hail ball radius was set to 20 mm.

Table 1 Geometric parameters of the finite element model of the honeycomb-reinforced PV module [29]

Structural component / Material	Thickness [mm]	Density [kg/m^3]	Young's modulus [GPa]	Poisson coefficient
PET	0.22	1400	2	0.37
EVA	0.5	950	0.08	0.4
Solar cell	0.17	2330	130	0.24
Honeycomb (PP)	12	120	1	0
ICE Ball	20	917	0.5	0.4

Experimental modal analysis was performed using a dedicated vibration test setup. Each flexible PV module reinforced with a honeycomb sandwich structure was mounted onto a specially designed aluminum frame. The edges of the module were fixed using mechanical clamps, ensuring repeatable boundary conditions while allowing free dynamic response in the out-of-plane (vertical) direction [30].

The clamped module-frame system was attached to a vibration test stand. Excitation was provided through a controlled vibration source powered by a signal generator and a power amplifier. Structural vibrations were measured using a combination of sensors, including two non-contact displacement sensors and the measurement system Lion Precision ECL202 equipped with a U3 sensor, enabling high-resolution response acquisition without introducing additional mass effects.

The experimental response was recorded in the frequency domain and time domain. The obtained signals were further processed to identify resonance peaks and estimate modal parameters.

In addition to conventional excitation-based modal testing, Operational Modal Analysis (OMA) was applied using Brüel & Kjær Operational Modal Analysis Pro software. OMA is particularly useful when the excitation is broadband or unknown, and modal parameters are extracted only from the measured response data [31].

For OMA implementation, a reference (control) measurement point was selected. The reference point was chosen to avoid nodal regions and extreme deformation zones, ensuring that it could reliably capture vibration response across multiple modes. A spatial grid of measurement points was defined on the PV module surface, and the grid geometry was represented in a three-dimensional coordinate system within the software environment.

During the test, the structure was excited by the shaker input and/or low-level broadband excitation. For each measurement, the vibration response of the reference point and one selected grid point was recorded. The modal properties were extracted using frequency-domain decomposition techniques embedded in the software.

OMA measurements were performed using two accelerometers, allowing the extraction of stable modal estimates in terms of natural frequencies, damping ratios, and mode shapes.

The key experimental outputs of the modal analysis are the Frequency Response Functions (FRFs). FRFs describe the relationship between input excitation and structural response in the frequency domain, enabling identification of resonance peaks and dynamic stiffness behavior.

The FRFs were used to determine:

- natural frequencies (f_n) as resonance peaks,
- modal damping ratio (ζ) from peak bandwidth or curve fitting techniques,
- mode shapes from the relative amplitudes and phase relationships across measurement points.

In this study, the FRF-based approach was essential to ensure that the extracted modal parameters could be directly compared to FE modal predictions, which are naturally expressed in terms of eigenfrequencies and eigenvectors [32].

A three-dimensional finite element (FE) model of the PV module with honeycomb reinforcement was developed to perform numerical modal analysis. The model included the main structural layers of the PV module and the honeycomb sandwich reinforcement, ensuring that stiffness and mass distributions were realistically represented.

The FE model was used to calculate eigenfrequencies and mode shapes.

Initial material properties were assigned based on manufacturer data and literature sources. Boundary conditions were implemented to replicate the experimental clamping conditions. However, since boundary conditions strongly influence modal parameters, especially for lightweight flexible structures, an iterative updating procedure was applied based on correlation results.

Since damping strongly affects the dynamic response under transient loading, experimentally extracted modal damping ratios (ζexp) were compared across repeated tests to ensure repeatability and reliability.

The modal damping ratio ζ was estimated using the Enhanced Frequency Domain Decomposition (EFDD) method, which extends conventional frequency-domain decomposition by enabling damping identification from operational response data. First, the cross-power spectral density matrix $S_{yy}(\omega)$ was computed from the measured vibration responses, and singular value decomposition (SVD) was applied at each frequency line. The dominant mode was identified from the peak of the first singular value spectrum, and a frequency band around the resonance was selected where a single mode contribution was dominant. The extracted spectral component was then transformed into the time domain using inverse Fourier transform, yielding an approximation of the impulse response function. The modal damping ratio was finally determined from the exponential decay of the reconstructed free vibration response using the logarithmic decrement method, while averaging over multiple cycles to reduce noise sensitivity.

The combined experimental–numerical modal analysis framework established in this study provides a reliable basis for dynamic modeling of next-generation honeycomb-reinforced lightweight PV modules. The validated FE model ensures that impact simulations (hail loading) are grounded in experimentally confirmed dynamic characteristics, enabling accurate prediction of stress concentration zones and supporting structural optimization aimed at improving module durability without compromising flexibility.

To ensure the reliability of the identified modal parameters and to quantify experimental uncertainty, modal testing was conducted on six nominally identical flexible PV modules reinforced with honeycomb sandwich structures. The use of multiple specimens allowed evaluation of repeatability and provided a statistical basis for distinguishing structural variability from measurement noise.

Repeatability was assessed by comparing the extracted modal parameters (natural frequencies, mode shapes, and modal damping ratios) across all tested modules. The dispersion of eigenfrequencies was quantified using statistical indicators such as the mean value and standard deviation, enabling evaluation of manufacturing-induced differences (e.g., adhesive layer thickness variations, honeycomb core imperfections, and laminate inhomogeneity). In addition, modal damping ratios were monitored across repeated measurements, as damping is typically more sensitive to boundary conditions and material nonlinearity than eigenfrequency estimates.

Measurement uncertainty was further influenced by experimental boundary conditions, including clamp stiffness and mounting repeatability, as well as sensor-related factors such as noise level, alignment errors, and sensitivity limitations. To minimize systematic errors, identical mounting procedures and consistent excitation settings were applied for all specimens. Furthermore, the use of non-contact displacement sensors reduced mass-loading effects and improved the accuracy of dynamic response measurements.

A simplified three-dimensional FE model of the flexible photovoltaic (PV) module reinforced with a honeycomb sandwich structure was developed using COMSOL Multiphysics in order to predict its dynamic characteristics and to support the interpretation of experimental modal analysis results. The main objective of the numerical model was to determine the module's natural frequencies and mode shapes, and to validate it against experimentally identified vibration modes prior to hail impact simulations.

The FE model included the main structural layers of the flexible PV module: the polymer frontsheet (terephthalate-based film), encapsulation layers, silicon solar cell layer, and polymer backsheet. The honeycomb reinforcement was represented using an equivalent structural layer approach, where the honeycomb core was modeled as an orthotropic medium to reduce computational cost while maintaining realistic stiffness distribution. The simplified model geometry was constructed based on the measured module dimensions and layer thicknesses. The developed model is shown schematically in Fig. 2.

Two separate FE models were employed in this study. A three-dimensional FE model was developed for modal analysis in order to capture the global bending and torsional deformation modes of the honeycomb-reinforced PV module and to validate the numerical stiffness representation against experimental modal data. Subsequently, a simplified two-dimensional cross-sectional FE model was adopted for transient hail impact simulations. The 2D model represented the through-thickness multilayer structure and was used to evaluate stress wave propagation and local stress concentrations under impact loading. This dimensional reduction substantially reduced computational cost while preserving the key stress-transfer mechanisms relevant to comparative assessment of reinforced and non-reinforced module configurations.

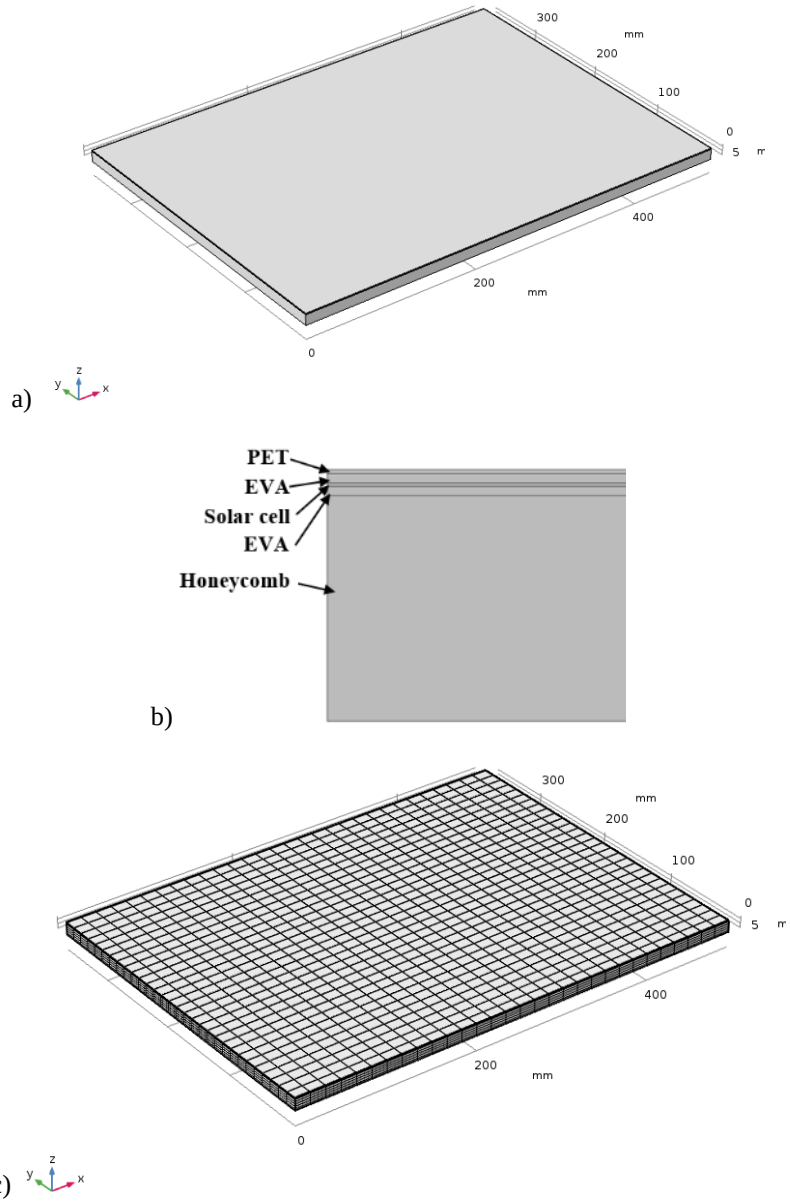


Fig. 2 Finite element model of the flexible PV module in COMSOL Multiphysics: (a) 3D view; (b) multilayer structural composition; (c) finite element discretization

All layers were assumed to behave as linear elastic materials, since the modal analysis was performed within a low deformation regime [33, 34]. The material parameters used in the FE model were obtained from manufacturer datasheets and literature sources. The main modeling parameters are summarized in Table 2.

Table 2 Geometric parameters of the FE model of the honeycomb-reinforced PV module

Parameter	Value [mm]
h_1	13.39
h_2	0.22
h_3	0.5
h_4	0.17
l	500
p	380
h_5	0.5

The polymer encapsulation layer was modeled as a homogeneous elastic medium with reduced Young's modulus to account for its compliant nature. The silicon solar cell layer was modeled as a thin brittle plate with isotropic stiffness properties. The terephthalate film and backsheet were treated as isotropic polymer layers.

The honeycomb reinforcement layer was implemented as an orthotropic equivalent material defined by three Young's moduli (E_x, E_y, E_z), shear moduli (G_{xy}, G_{yz}, G_{xz}), and Poisson ratios. This approach allowed capturing the anisotropic stiffness contribution of the honeycomb core without explicitly modeling its cellular geometry.

To ensure consistency with the experimental modal analysis, the numerical boundary conditions were designed to replicate the test mounting configuration. The PV module edges were constrained at the clamping regions, assuming fixed displacement in the out-of-plane direction, while allowing limited in-plane movement depending on clamp compliance.

In the model, the clamped boundary condition was represented by fixed constraints applied to the module edges along the frame contact surfaces. This approximation was selected as a conservative representation of the experimental setup. Since boundary conditions strongly influence natural frequencies, a sensitivity check was performed by varying the clamp stiffness in the model. The best agreement with experimental frequencies was obtained using partially constrained boundary conditions, indicating that the experimental clamps exhibit finite compliance.

The FE mesh consisted of tetrahedral elements with local refinement in regions of expected high curvature and stiffness transitions, particularly near the solar cell boundaries and clamping zones. A mesh convergence study was performed to ensure that the eigenfrequency results were not affected by discretization errors. The final mesh contained 9,450 elements and 11,160 nodes, resulting in stable eigenfrequency predictions with less than 1% variation between successive mesh refinements.

Modal analysis was performed using the Eigenfrequency study module in COMSOL. The first six natural frequencies were extracted within the frequency range of 0–500 Hz, corresponding to the range used in experimental measurements. The solver employed an iterative eigenvalue algorithm with relative tolerance set to 10^{-6}, ensuring numerical stability and accurate mode extraction.

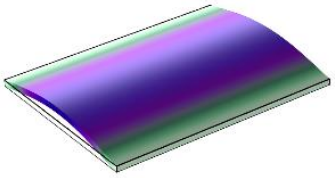
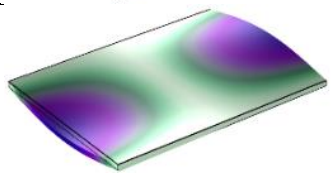
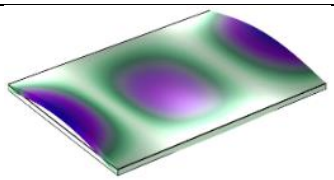
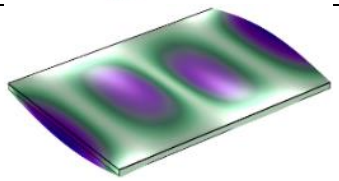
3. RESULTS

The FE simulation results (Table 3) revealed a set of global eigenmmodes consistent with experimental observations. The first mode corresponded to a global out-of-plane bending deformation with maximum displacement located at the module center. The

second mode was identified as a torsional mode around the longitudinal axis, while the third and fourth modes exhibited mixed bending–torsion behavior with partial deformation localization near the clamped edges.

The predicted eigenfrequencies were found to be in close agreement with experimental results. For example, the FE model predicted the first natural frequency at $f_{1,FE}$ = 165.12 Hz, compared to the experimentally measured value $f_{1,exp}$ = 156 Hz, resulting in a relative deviation of 5.52%. Similarly, the deviations for the first four modes remained below 10%, with the first, second, and fourth modes showing deviations of approximately 5.5%, 4.5%, and 6.7%, respectively, while the third mode exhibited a higher deviation of 9.8%, indicating that the FE model captures the overall stiffness and mass distribution of the flexible PV module.

Table 3 Comparison of modal analysis of a flexible PV module

Mode	Frequency [Hz]	Shape form
1	165.12	
2	195	
3	295	
4	482.5	

The simulated mode shapes also matched the experimentally identified deformation patterns. In particular, the highest displacement amplitudes were observed in the internal region of the PV module, confirming that the global dynamic response is dominated by bending deformation rather than edge-dominated vibration. This observation is consistent with the experimental modal analysis, where maximum vibration amplitudes were recorded at the central surface measurement points.

The validated numerical model confirms that honeycomb reinforcement significantly influences the global stiffness of the flexible PV module, shifting the dominant bending

and torsional modes into higher frequency ranges compared to non-reinforced flexible laminates. The predicted displacement fields indicate that the highest dynamic deformation occurs in the central module area, which is expected to be the most critical zone under transient mechanical loading such as hail impact.

The numerical model therefore provides a reliable foundation for subsequent transient dynamic simulations, where experimentally identified modal damping ratios can be introduced to represent realistic energy dissipation. Moreover, the FE model enables further parametric studies investigating the influence of honeycomb thickness, equivalent stiffness properties, and encapsulation layer modulus on the dynamic response and impact resistance of next-generation lightweight PV modules.

The dynamic characteristics of the flexible photovoltaic (PV) module reinforced with a honeycomb sandwich structure were identified through experimental and numerical modal analysis. The main objective was to determine the natural frequencies, mode shapes, and damping ratios of the module and to validate the developed finite element (FE) model for subsequent hail impact simulations.

Fig. 3a presents the experimentally obtained Frequency Response Functions (FRFs) of the tested module, where distinct resonance peaks were observed within the frequency range of 0–600 Hz. The first dominant resonance occurred at approximately f_1 = 156 Hz, followed by higher vibration modes at f_2 = 182.5 Hz, f_3 = 269 Hz, and f_4 = 456 Hz. The resonance peaks were consistent across repeated measurements, confirming stable structural behavior and sufficient measurement quality.

The corresponding mode shapes were extracted and classified based on their deformation patterns. The first mode was identified as a global bending mode in the out-of-plane direction, characterized by maximum deflection near the module center. The second mode exhibited a torsional deformation, indicating twisting around the longitudinal axis. The third and fourth modes showed combined bending–torsion behavior, with localized deformation zones near the clamped edges, suggesting boundary-condition sensitivity and stiffness discontinuities related to the honeycomb reinforcement and lamination interfaces.

Figs. 3a and 3b present the experimentally obtained Frequency Response Functions (FRFs) measured at two different locations of the photovoltaic module: the center measurement point and the measurement point located at the middle of the module edge, respectively. These FRFs were used to identify the natural frequencies and to verify the consistency of the dynamic response at different locations of the structure. Fig. 3c illustrates the determination of the first modal damping ratio using the Enhanced Frequency Domain Decomposition (EFDD) method. The damping ratio of the first mode was approximately ζ_1 = 1.577 %, while higher modes exhibited lower damping levels, typically within the range of 0.8–1.5%. The observed damping behavior is attributed to viscoelastic dissipation in polymeric layers and interfacial friction effects in the sandwich structure. These results highlight the significant role of polymeric materials and bonding quality in governing energy dissipation mechanisms.

To evaluate repeatability, modal testing was performed on six nominally identical PV modules. The identified natural frequencies showed low scatter, with the coefficient of variation (COV) remaining below 3% for the first four modes. For instance, the first natural frequency exhibited an average value of 156 Hz with a standard deviation of ±1.9 Hz, indicating that manufacturing variability had a limited influence on the global stiffness of the structure.

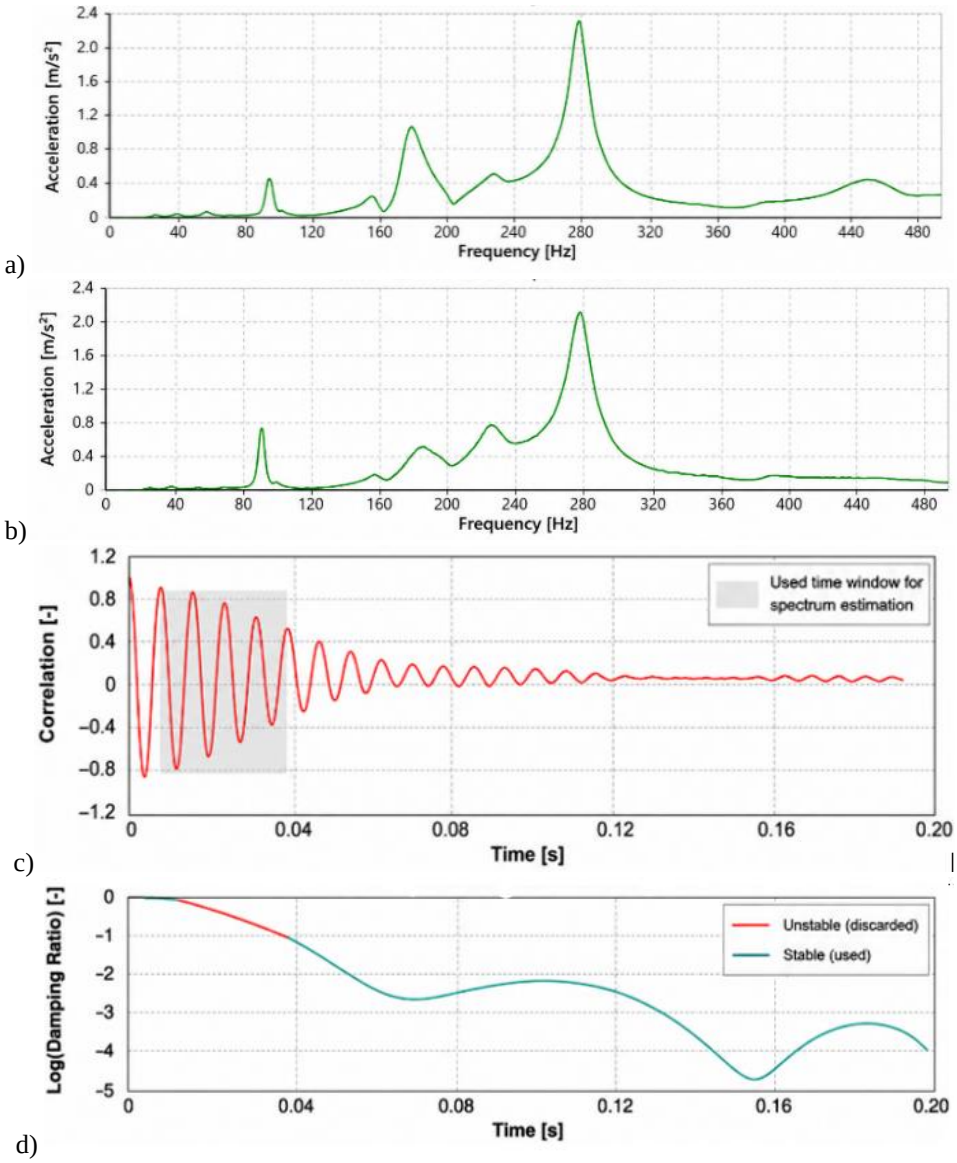
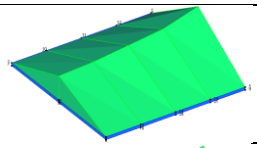
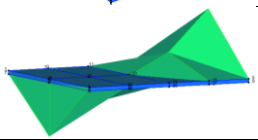
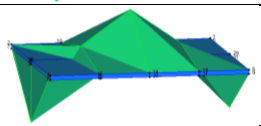
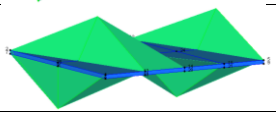


Fig. 3 Experimental modal analysis results of the honeycomb-reinforced PV module: a) Frequency Response Function (FRF) measured at the center point of the photovoltaic module; b) Frequency Response Function (FRF) measured at the point located on the middle edge of the photovoltaic module; c) Determination of the first mode modal damping ratio using the Enhanced Frequency Domain Decomposition (EFDD) method: (d) normalized correlation function of the selected singular value in the time domain (see c)) and validation of the first modal damping ratio estimate.

In contrast, modal damping ratios demonstrated higher variability between specimens, with a COV reaching up to 10–15%, which is expected due to the sensitivity of damping to bonding conditions, polymer aging effects, and clamping repeatability. Nevertheless, the overall trends remained consistent, confirming that the identified damping ratios can be used as representative values for transient impact simulations.

The experimentally extracted modal parameters were compared with the FE model predictions. Table 4 summarizes the experimental and numerical natural frequencies, frequency deviations values for the first four modes. The FE model predicted the first natural frequency as $f_{1,FE}$ = 165.12 Hz, resulting in a frequency deviation of 5.52%. Similarly, deviations for the second, third, and fourth modes were below 6%, indicating good agreement between numerical and experimental results.

Table 4 Comparison of modal analysis of a flexible PV module

Mode	Frequency, f_{exp} (Hz)	Damping Ratio, ζ (%)	Theoretical f_{FE} (Hz)	Δf (%)	Shape form
1	156	1.577	165.12	5.52	
2	182.5	1.519	195	4.5	
3	269	1.865	295	9.8	
4	456	1.240	482.5	6.7	

The validated FE model therefore provides a reliable representation of the PV module dynamic behavior and was considered suitable for subsequent dynamic impact simulations. The agreement between experiment and simulation confirms that the honeycomb sandwich reinforcement significantly increases structural stiffness, shifting resonance frequencies into higher ranges compared to conventional flexible PV laminates reported in previous studies.

The obtained modal parameters indicate that the flexible honeycomb-reinforced PV module exhibits dominant global bending and torsional modes within the low-frequency range. Since hail impact represents a short-duration transient load with high-frequency content, the validated FE model is essential for capturing the dynamic stress redistribution during impact. In particular, the identified mode shapes suggest that the module center region and the clamped boundary areas are the most critical zones, where peak stresses are likely to occur during dynamic excitation.

Additionally, the experimentally determined damping ratios provide important input data for transient simulations, enabling more realistic prediction of stress attenuation and vibration decay following impact. Overall, the modal analysis results confirm that the proposed honeycomb reinforcement concept improves dynamic stiffness and provides a stable mechanical platform for lightweight PV applications under extreme environmental loading.

4. DISCUSSION

The obtained modal analysis results confirm that the flexible PV module reinforced with a honeycomb sandwich structure exhibits clearly distinguishable global bending and torsional modes within the low-frequency range, which is characteristic of lightweight laminated composite systems. In comparison with Corrado et al. (2017), who investigated flexible PV laminates under simulated hail impacts and emphasized the strong influence of boundary conditions and laminate mechanical properties on the dynamic response, the present study similarly demonstrates increased sensitivity of higher-order modes to clamping stiffness and edge constraints. Furthermore, the experimentally identified modal damping ratios indicate that energy dissipation is mainly governed by the viscoelastic behavior of polymer encapsulation layers and interfacial effects, which is consistent with previous findings for polymer-based lightweight PV concepts. Schüler et al. (2024) highlighted that next-generation lightweight VIPV modules with fiber-reinforced front sheets can significantly improve structural stiffness and impact resistance; however, reliable implementation requires validated numerical models capable of capturing dynamic behavior. In this study, the strong agreement between experimental and FE modal parameters (low frequency deviations) confirms that honeycomb reinforcement not only enhances stiffness but also enables the development of a robust validated FE model suitable for subsequent hail impact simulations and structural optimization.

Following validation of the global dynamic behavior using the three-dimensional modal FE model, a separate two-dimensional cross-sectional FE model was developed for transient hail impact simulations in order to analyze through-thickness stress transfer under contact loading.

The hail impact response of the next-generation lightweight flexible photovoltaic (PV) module reinforced with a honeycomb sandwich structure was investigated using numerical simulation in COMSOL Multiphysics. The finite element model was developed based on the validated modal analysis results presented in Section 3.1, ensuring that the dynamic stiffness distribution and boundary condition representation correspond to the experimentally observed structural behavior. This validation step was essential to obtain realistic stress wave propagation and load transfer through the multilayer PV module under transient impact loading.

The numerical study aimed to simulate the transmission of hail impact force through the PV module layers and to evaluate the critical stress concentrations responsible for microcrack initiation and potential structural failure. A contact-based damage formulation was implemented to represent the interaction between the hailstone and the PV module surface. The formulation included a damage variable associated with local penetration and contact pressure evolution, enabling assessment of surface layer degradation under high-rate impact conditions.

To evaluate the mechanical response, the von Mises equivalent stress criterion was selected as the primary indicator of structural integrity. Although brittle materials such as silicon typically fail under tensile stresses, the von Mises stress provides a robust engineering measure for comparing stress levels within multilayer systems and identifying regions of maximum stress accumulation. This criterion is widely applied in PV reliability studies and provides a conservative estimation of stress concentration zones where microcracks may occur.

A two-dimensional (2D) FE model was adopted to reduce computational effort while maintaining sufficient accuracy for comparative stress analysis. The model consisted of a spherical ice projectile (hailstone) with a radius of 20 mm and a representative segment of the flexible PV module with a width of 20 mm, including the main structural layers. The honeycomb reinforcement was represented through an equivalent stiffness layer, capturing the effect of the sandwich back structure on the impact response.

To allow clear observation of the impact process and avoid initial numerical instability, an initial gap of 1 mm was defined between the hailstone and the PV module surface. The layer thicknesses and material properties applied in the simulation are summarized in Table 1.

The FE mesh was generated with consideration of the geometry complexity and contact region resolution. The hailstone was discretized using 419 triangular elements, while the PV module segment was discretized using 950 quadrilateral elements, resulting in a total of 1257 nodes. Mesh refinement was applied in the expected contact area to improve stress prediction accuracy. The PV module mounting region was fixed at the bottom boundary (highlighted in red in Fig. 4), representing the constrained support conditions during standardized testing.

Fig. 4a illustrates the general view of the 2D impact simulation setup, while Fig. 4b presents the main components of the model. The FE discretization is shown in Fig. 4c.

Two theoretical cases were investigated for the hail impact simulation: the first case included the honeycomb structure (corresponding to Fig. 5a and Fig. 5c), while the second case was modeled without the honeycomb reinforcement (corresponding to Fig. 5b and Fig. 5d).

The numerical simulation results indicate that the impact generates a high compressive stress wave at the contact interface, followed by stress wave propagation through the multilayer structure. The maximum von Mises stress values were concentrated near the impact point on the front layer and subsequently transferred into deeper layers, including the encapsulation and solar cell region. This behavior confirms that the mechanical response of flexible PV modules is strongly dependent on the stiffness gradient between layers and the ability of the encapsulation material to redistribute impact energy.

Fig. 5 presents the numerical simulation results of hail impact on a flexible PV module under two structural configurations: with honeycomb reinforcement (Figs. 5a and 5c) and without honeycomb reinforcement (Figs. 5b and 5d). Figures 5a and 5b show the von Mises stress distribution fields obtained immediately after impact, together with a magnified view of the contact region between the hailstone and the PV module layers. Figures 5c and 5d provide the corresponding von Mises stress profiles through the module thickness, clearly indicating stress propagation across the PET, EVA, solar cell, and supporting layers.

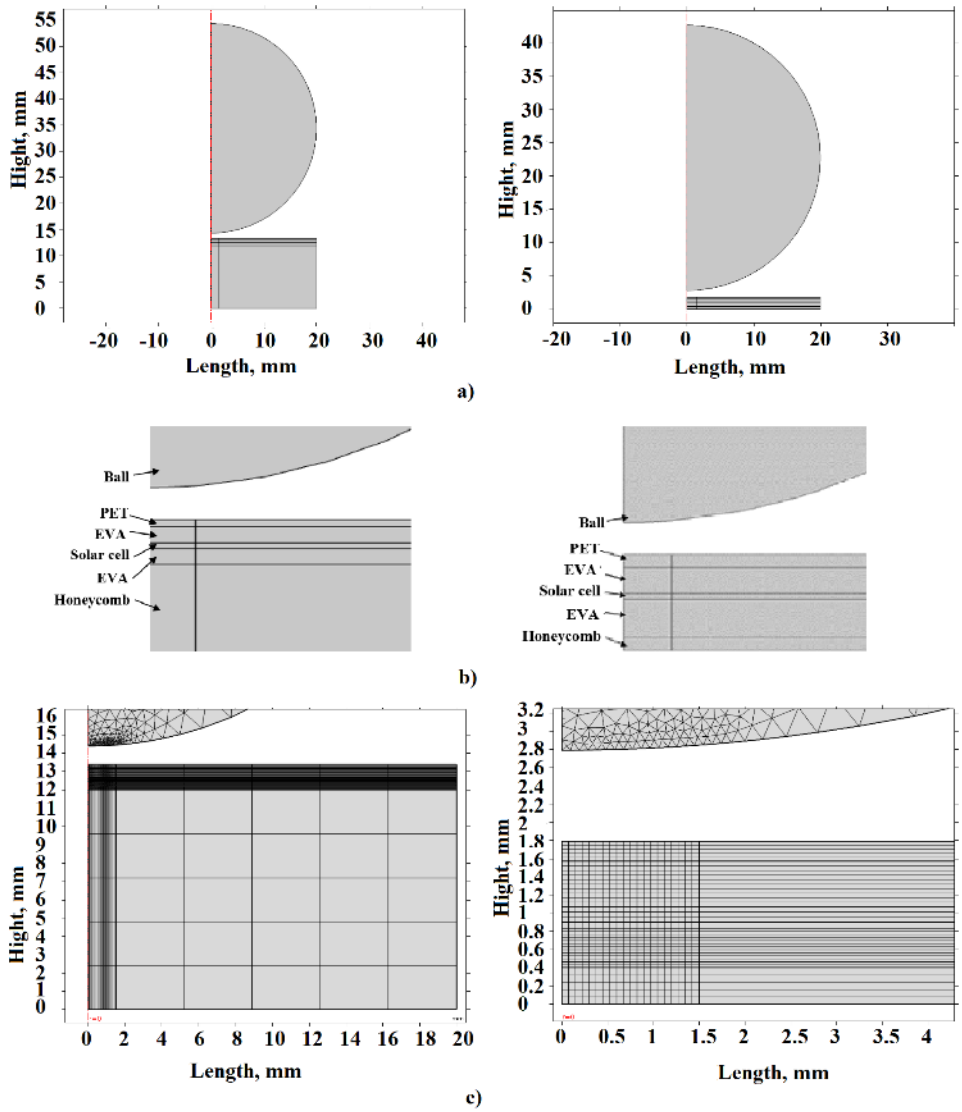


Fig. 4 Simulation of hail impact on flexible PV modules:
a) General view; b) Materials; c) FE mesh for simulation of hail impact

The results reveal that the highest stresses were concentrated near the impact zone and within the brittle solar cell layer. For the PV module without honeycomb reinforcement (Fig. 5b and Fig. 5d), the von Mises stress values in the solar cell layer ranged from 9000 kPa to 146500 kPa. The results reveal that the highest stresses were concentrated within the brittle solar cell layer beneath the impact zone. For the PV module without honeycomb reinforcement (Fig. 5b and Fig. 5d), the peak von Mises stress reached approximately 146.5 MPa. In contrast, the honeycomb-reinforced configuration (Fig. 5a and Fig. 5c) exhibited a

slightly higher peak stress of approximately 149.8 MPa. This increase is attributed to the higher global stiffness of the sandwich-supported structure, which reduces overall deformation but promotes more direct stress transfer into the brittle silicon layer during transient impact loading.

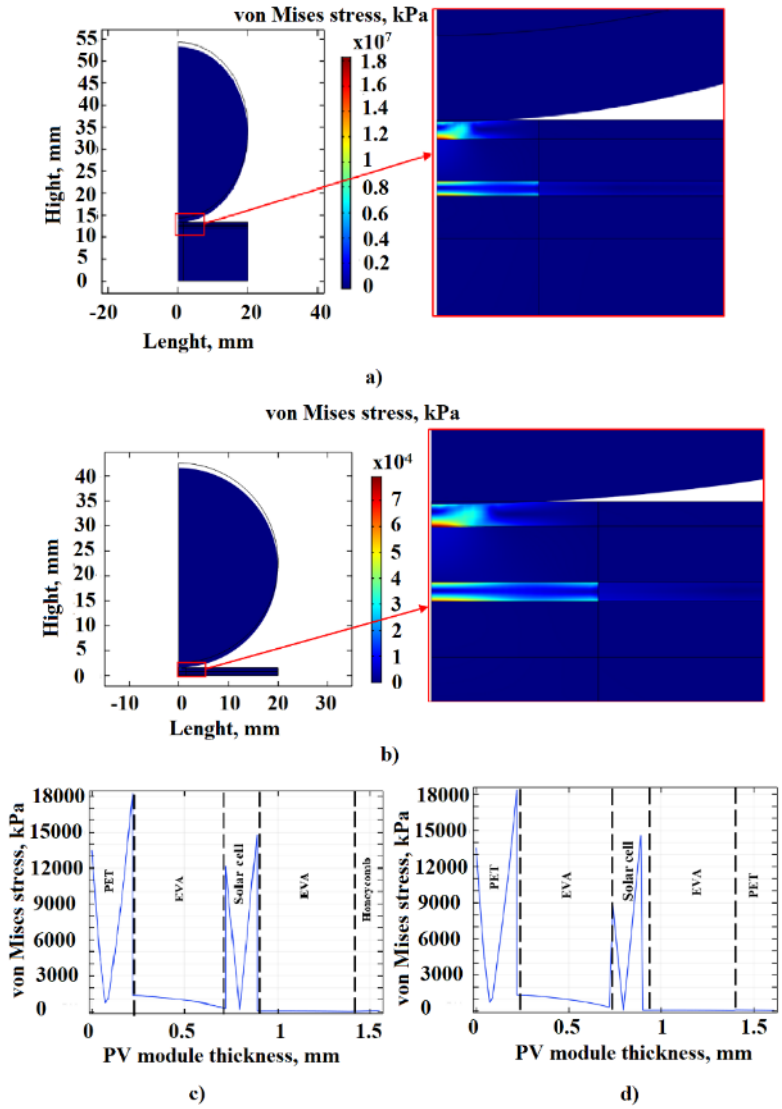


Fig. 5 Hail impact simulation results for flexible PV modules: (a) von Mises stress distribution with honeycomb reinforcement; (b) von Mises stress distribution without reinforcement; (c) through-thickness stress profile with honeycomb; (d) through-thickness stress profile without honeycomb.

The results also revealed that the honeycomb reinforcement significantly alters the load transfer path by increasing the global bending stiffness of the module segment. Consequently, stress localization in the solar cell layer was reduced compared to conventional flexible laminate designs reported in previous studies. The most critical region was identified at the interface between the encapsulation layer and the brittle solar cell material, where tensile stress components occur during rebound and bending recovery. This stress reversal mechanism is known to be a primary cause of microcrack formation in PV cells.

In addition, high stress gradients were observed near the module support boundary, indicating that boundary conditions influence the dynamic response and may contribute to crack initiation if the module is rigidly constrained.

The simulation results demonstrate that the honeycomb sandwich reinforcement improves the mechanical resistance of lightweight flexible PV modules by increasing stiffness and reducing the magnitude of stress transferred into the solar cell layer. This finding supports the concept that honeycomb-based reinforcement is an effective design strategy for next-generation PV modules intended for applications where weight reduction is critical, such as building-integrated photovoltaics (BIPV) and vehicle-integrated photovoltaics (VIPV).

Furthermore, the validated FE model provides insight into the influence of layer thickness and material properties on impact stress distribution. Increasing the thickness of the front protective polymer layer results in lower peak stresses in the solar cell region due to improved impact energy absorption and delayed stress wave transmission. Conversely, reducing the thickness of the lower lamination layer decreases overall stiffness but improves flexibility, indicating that an optimized trade-off between mechanical resistance and structural adaptability is required.

Overall, the hail impact simulations confirm that the highest probability of failure is associated with microcrack initiation in the solar cell layer, which is consistent with experimentally observed PV degradation mechanisms. The numerical findings also highlight the importance of using validated dynamic models, since incorrect stiffness representation can significantly distort stress predictions and lead to unreliable conclusions about module durability.

The developed 2D impact simulation framework represents the standardized hail impact scenario typically applied in PV reliability testing. The model enables evaluation of stress evolution and identification of damage-sensitive zones without destructive testing. The obtained results provide a reliable basis for future parametric optimization studies, where honeycomb geometry, reinforcement thickness, and encapsulation material properties can be systematically varied to maximize hail resistance while maintaining lightweight and flexible characteristics.

Although the present study investigates hail-induced stress propagation in lightweight PV modules, the simulations were primarily intended for comparative structural assessment and dynamic response evaluation rather than direct IEC 61215 certification analysis. The standardized IEC 61215 hail test protocol typically employs a 25 mm ice ball impacting at approximately 23 m/s under prescribed testing conditions. Therefore, the stress values obtained in the present work should be interpreted as relative indicators of structural behavior and stress transfer efficiency rather than direct pass/fail certification criteria. Future work should extend the validated FE framework toward full IEC-compliant

impact conditions, including standardized projectile dimensions, velocities, and experimentally verified failure thresholds.

The numerical results indicate that the flexible PV module reinforced with a honeycomb sandwich structure exhibits slightly higher von Mises stress levels in the solar cell layer compared to the configuration without honeycomb reinforcement. This behavior can be explained by the increased global stiffness of the honeycomb-supported structure, which reduces overall bending deformation under impact loading but simultaneously increases the effective contact stiffness during the transient event. Therefore, a larger portion of the impact energy is transferred directly into the brittle silicon layer instead of being dissipated through global deflection and viscoelastic deformation of polymeric encapsulation layers. In addition, the honeycomb core acts as a rigid support, limiting the structural compliance of the laminate and promoting localized stress concentration in the cell region. This effect is consistent with the dynamic response of sandwich structures, where enhanced stiffness improves structural stability but may amplify peak stress transmission into sensitive layers under high-rate loading. Therefore, while honeycomb reinforcement is beneficial for improving the overall mechanical integrity and reducing global displacement, further optimization of intermediate layers (e.g., EVA thickness, compliant interlayers, or graded stiffness transition zones) is required to mitigate stress peaks in the solar cell and enhance impact resistance under standardized hail conditions.

Since mounting stiffness strongly affects the global dynamic response of lightweight PV modules, the probability of microcrack initiation under hail impact may differ considerably between laboratory and field installations. Rigid mounting conditions tend to increase localized stress transfer into brittle silicon layers due to reduced global deformation, whereas more compliant support systems may partially redistribute impact energy through larger structural deflections. Consequently, real-world support configurations may substantially influence crack initiation behavior and should be considered in future parametric studies involving realistic installation conditions and support flexibility variations.

Although the von Mises equivalent stress criterion provides a convenient engineering measure for comparative assessment of stress concentration and load transfer within multilayer PV structures, it does not fully represent brittle fracture behavior in silicon solar cells. Microcrack initiation in brittle materials is more strongly governed by localized tensile principal stresses, particularly during rebound and bending recovery phases following impact. Consequently, the present approach may underestimate local crack-initiation sensitivity in regions subjected to transient tensile stress peaks. Future studies should therefore incorporate maximum principal stress evaluation and fracture-mechanics-based failure criteria to improve prediction accuracy for brittle-cell damage initiation and propagation.

Although the honeycomb core was represented as an equivalent homogenized orthotropic layer, this modeling approach does not resolve local stress concentrations associated with individual honeycomb cell walls, cell-wall junctions, or possible manufacturing defects such as non-uniform adhesive thickness, partial debonding, or imperfect bonding between the core and face sheets. Therefore, the present model should be interpreted as a global and comparative dynamic assessment rather than a detailed local damage prediction tool. Future studies should incorporate explicit honeycomb cell geometry and cohesive-zone or contact-based interface models to evaluate local stress hot spots and defect-induced failure mechanisms.

5. CONCLUSION

This study investigated the dynamic behavior and hail impact resistance of a next-generation lightweight photovoltaic (PV) module reinforced with a honeycomb sandwich structure. The increasing demand for lightweight PV solutions in building- and vehicle-integrated applications necessitates structurally efficient alternatives to conventional glass-based modules, which are often limited by excessive mass and rigidity.

An integrated experimental–numerical methodology was developed and applied. Experimental modal analysis enabled identification of the key dynamic parameters of the honeycomb-reinforced flexible PV module, including natural frequencies, mode shapes, and modal damping ratios. The developed finite element (FE) model demonstrated good agreement with experimental results, with eigenfrequency deviations remaining below 10% for the first four modes, although the third mode showed a comparatively higher deviation of 9.8%, confirming that the stiffness distribution and boundary conditions were adequately represented.

The validated FE model was subsequently employed for transient hail impact simulations. The results showed that the highest von Mises stresses were consistently concentrated within the brittle silicon solar cell layer, indicating that microcrack initiation remains the primary failure mechanism under impact loading. The honeycomb reinforcement increased global structural stiffness and reduced overall deformation; however, this stiffness enhancement also resulted in slightly higher localized stress peaks in the solar cell layer due to more direct stress transmission.

The findings highlight a critical trade-off between global stiffness improvement and local stress amplification in sandwich-reinforced lightweight PV modules. While honeycomb reinforcement enhances structural stability and mechanical robustness, further optimization of intermediate compliant layers is required to mitigate stress concentration in brittle functional components.

Acknowledgement: *This project has received funding from the Research Council of Lithuania (LMTLT), agreement No S-PD-24-129.*

REFERENCES

1. Wang, Z., Liu, S., Li, J., Cao, S.-J., 2026, *Climate drivers of photovoltaic degradation: Regional variability and material pathways*, Applied Energy, 410, 127555.
2. Pryor, S.C., Barthelmie, R.J., 2026, *Hail as a damage vector for renewable energy*, iScience, 29(1), 114439.
3. Vergil, H., Mursal, M., Kaplan, M., Khan, A.U.I., 2024, *The Causal Relationship between Public Investment in Renewable Energy and Climate Change Performance Index*, International Journal of Energy Economics and Policy, 15(1), pp. 121–130.
4. Mateko, F. M., Vutula, N., 2024, *Disaster induced displacement and durable solutions in Africa*, Natural Hazards, 120(15), pp. 13835–13849.
5. Erhart, S., Szabó, S., Erhart, K., 2025, *Integrating Pollutant registers for the climate change risk evaluation of industrial companies in Australia, Europe and North America*, Scientific Reports, 15(1), 1207.
6. Liao, H., Ye, H., 2023, *Endogenous economic structure, climate change, and the optimal abatement path*, Structural Change and Economic Dynamics, 65, pp. 417–429.
7. Mannino, G., Battaglioli, F., Tina, G.M., 2026, *Large hail impacts on photovoltaic systems: A review of damage, testing, and mitigation*, Energy Reports, 15, 109056.

8. Ayadi, O., Shadid, R., Bani-Abdullah, A., Alrbai, M., Abu-Mualla, M., Balah, N., 2022, *Experimental comparison between Monocrystalline, Polycrystalline, and Thin-film solar systems under sunny climatic conditions*, Energy Reports, 8, pp. 218–230.
9. Forni, D., Caccivio, M., Chudy, D., Cadoni, E., 2025, *An experimental investigation of ice ball impact behaviour to improve PV panel hailstone safety*, International Journal of Impact Engineering, 202, 105315.
10. Chakraborty, S., Haldkar, A. K., Manoj Kumar, N., 2023, *Analysis of the hail impacts on the performance of commercially available photovoltaic modules of varying front glass thickness*, Renewable Energy, 203, pp. 345–356.
11. Hartley, J. Y., DiGregorio, S., Weil, J., Zhang, K., Braid, J. L., 2024, *Analyzing Hail Impact-Induced Glass Fracture in Photovoltaic Modules Using High Speed Video and Computational Simulation*, In 2024 IEEE 52nd Photovoltaic Specialist Conference (PVSC), Seattle, WA, USA, pp. 1676–1678.
12. Depiver, J. A., Mallik, S., Harmanto, D., 2021, *Solder joint failures under thermo-mechanical loading conditions – A review*, Advances in Materials and Processing Technologies, 7(1), pp. 1–26.
13. Nicoletto, M., Panizzon, D., Caria, A., Trivellin, N., De Santi, C., Buffolo, M., Meneghini, M. ,2025, *Hail Damage Investigation in Heterojunction Silicon Photovoltaic Modules: A Real-World Case Study*, IEEE Journal of Photovoltaics, 15(3), pp. 478–483.
14. Chen, X., Karin, T., Jain, A., 2025, *Analyzing the impact of design factors on solar module thermomechanical durability using interpretable machine learning techniques*, Applied Energy, 377, 124462.
15. Ali, H. B., Kamran, M.A., Gul, R.M., Yasir, M., Alabdullah, F.T., Usman, C., Tariq, A., 2024, *Mechanical integrity of photovoltaic panels under hailstorms: Mono vs. poly-crystalline comparison*, Heliyon, 10(4), 25865.
16. DiGregorio, S. J., Braid, J. L., Shimizu, M., Hartley, J. Y., 2024, *Laboratory Hail Damage of Photovoltaic Modules: Electroluminescence and High-speed Digital Image Correlation Analysis*, In 2024 IEEE 52nd Photovoltaic Specialist Conference (PVSC), Seattle, WA, USA, pp. 1625–1628.
17. Jiao, B., Fang, Q., Liu, C., Zhang, Y., Shen, Y., Shen, Y., Guo, A., 2026, *Numerical investigation of crack propagation in PV modules with initial micro-cracks*, Solar Energy Materials and Solar Cells, 297, 114120.
18. Fang, Q., Jiao, B., Yu, D., Liu, C., Liu, P., 2026, *Investigation of fatigue crack propagation in photovoltaic modules under dynamic cyclic loading*, Solar Energy, 304, 114217.
19. Shi, Z., Liu, Z., Zhang, T., Dong, Y., Hong, H., Yang, Y., Cai, J., 2025, *Mechanical performance analysis of the lightweight semi-flexible photovoltaic module*, Energy, 335, 138151.
20. Papargyri, L., Papanastasiou, P., Georghiou, G.E., 2024, *Sequential thermomechanical stress and cracking analysis of photovoltaic modules with full and half-cut cells*, Solar Energy Materials and Solar Cells, 278, 113166.
21. Milić, P., Marinković, D., Ćojbašić, Ž., 2025, *Geometrically nonlinear analysis of piezoelectric active laminated shells by means of isogeometric FE formulation*, Facta Universitatis-Series Mechanical Engineering, 23(2), pp. 387-405.
22. Paul, D., Devaprakasam, D., 2025, *Mitigating the impact of ultraviolet radiation and extreme environments on solar cell and panel performance: A state-of-the-art review and critical analysis*, Solar Energy, 290, 113342.
23. Zhang, G., Zheng, Y., Wang, H., Ding, G., Yang, F., Xu, Y., Shao, Y., 2024, *Shellac protects perovskite solar cell modules under real-world conditions*, Joule, 8(2), pp. 496–508.
24. Yadav, A., Kumar, A., K., M., 2025, *Performance impact of environmental and operational factors on solar photovoltaic panels*, Environmental Progress & Sustainable Energy, 44(6), 70062.
25. Nicoletto, M., Panizzon, D., Caria, A., Trivellin, N., De Santi, C., Buffolo, M., Meneghini, M., 2025, *Modeling Cracks in Silicon-Heterojunction Photovoltaic Modules: A Real-World Case Study*. IEEE Journal of Photovoltaics, 15(5), pp. 639–644.
26. Perry, K., Nguyen, Q., Jordan, D., 2025, *Automatically Calculating Hail and Hurricane Damage to Photovoltaic Systems in Satellite Imagery using Deep Learning Techniques*, In 2025 IEEE 53rd Photovoltaic Specialists Conference (PVSC), Montreal, QC, Canada, pp. 0270–0275.
27. Braid, J. L., Jost, N. R., Hartley, J. Y., Shimizu, M., Hansen, C. W., 2025, T*echnoeconomic Analysis of Robust PV Module Designs to Mitigate Glass Failure*. In 2025 IEEE 53rd Photovoltaic Specialists Conference (PVSC), Montreal, QC, Canada: IEEE., pp. 1437–1439.
28. Kuchak, A.J.T., Marinkovic, D., Zehn, M., 2021, *Parametric Investigation of a Rail Damper Design Based on a Lab-Scaled Model*, Journal of Vibration Engineering and Technologies, 9 (1), pp. 51-60.
29. Kilikevičienė, K., Matijošius, J., Fursenko, A., Kilikevičius, A., 2019, *Tests of hail simulation and research of the resulting impact on the structural reliability of solar cells*, Ekspolatacja i Niezawodnosc - Maintenance and Reliability, 21(2), pp. 275–281.

30. Kilikeviciene, K., Matijosius, J., Kilikevicius, A., Jurevicius, M., Makarskas, V., Caban, J., Marczuk, A., 2019, *Research of the Energy Losses of Photovoltaic (PV) Modules after Hail Simulation Using a Newly-Created Testbed*, Energies, 12(23), 4537.
31. Makarskas, V., Jurevicius, M., Zakis, J., Kilikevicius, A., Borodinas, S., 2019, *Simulation Study of Hail Impact on Photovoltaic Modules*, In 2019 IEEE 7th IEEE Workshop on Advances in Information, Electronic and Electrical Engineering (AIEEE), Liepaja, Latvia: IEEE., pp. 1–4.
32. Kilikevičius, A., Čereška, A., Kilikevičienė, K., 2016, *Analysis of external dynamic loads influence to photovoltaic module structural performance*, Engineering Failure Analysis, 66, pp. 445–454.
33. Borucka, A., Kozlowski, E., Oleszczuk, P., Mazurkiewicz, D., 2020, *The Use of Mathematical Models Describing the Spread of Covid-19 in Strategic State Security Management*, European Research Studies Journal, XXIII(Special 3), pp. 82–98.
34. Kozłowski, E., Borucka, A., Oleszczuk, P., Leszczyński, N., 2024, *Evaluation of readiness of the technical system using the semi-Markov model with selected sojourn time distributions*, Eksploatacja i Niezawodność – Maintenance and Reliability, 26(4), 191545.